FLOW IN AGGREGATE - BINDER MIXES

FEBRUARY 1970 - NUMBER 3

BY

E. TONS

W.H. GOETZ

V L. ANDERSON

JHRP

JOINT HIGHWAY RESEARCH PROJECT

PURDUE UNIVERSITY AND

INDIANA STATE HIGHWAY COMMISSION

Technical Paper

FLOW IN AGGREGATE - BINDER MIXES

by

Egons Tons, Associate Professor of Civil Engineering, University of Michigan

formerly Graduate Assistant, Purdue University

W. H. Goetz, Professor of Highway Engineering, Purdue University

V. L. Anderson, Professor of Statistics, Purdue University

Joint Highway Research Project

Project: C-36-6X
File: 2-4-24

Prepared as Summary of an Investigation Conducted by

Joint Highway Research Project
Engineering Experiment Station
Purdue University

in cooperation with the

Indiana State Highway Commission
and the

U. S. Department of Transportation
Federal Highway Administration
Bureau of Public Roads

For presentation at the Annual Meeting of the Association of Asphalt and Paving Technologists, February 9 - 11, 1970

Purdue University
Lafayette, Indiana
January 1970

INTRODUCTION

Prediction of field service behavior of a bituminous mix on the basis of its composition or material ingredients, presents a difficult problem. In spite of this, research and experience have provided methods for practical mix designs which are adequate in most cases.

The designs used at present are essentially trial and error in nature. The type and gradation of aggregate and the asphalt grade are chosen, then a number of asphalt contents are estimated which hopefully bracket the desired optimum conditions. Next follows the making of specimens and their testing to determine the optimum mix. If the combination of ingredients does not give the specified or desired properties (stability, voids, etc.), the components in the mix are changed and the tests are repeated.

The assumption at the start of this investigation was that a knowledge of physical factors of the aggregate and the binder could lead to a more systematic and unified mix design procedure.

PURPOSE AND SCOPE

The specific objectives of this research were:

a. To define and measure quantitatively useful mix-design parameters for aggregates.

b. To define and analyze the function of asphalt in a mix.

c. To try to predict "strength" values for aggregate-asphalt mixtures from composition parameters.

d. To initiate an approach to a unified mix design.

The initial hypothesis involved the assumption that, in order to achieve a more uniform approach in mix design, different types of aggregate, such as crushed limestone and rounded gravel, should be graded in such a manner that under identical circumstances the number of active particles and their "size" distribution would be identical in a given unit volume. When asphalt is added to rock particles, part of it will become bound to the valleys of the rock surfaces; the other part will be participating in the flow of a mix under load. The amount of the bound or stagnant asphalt should vary with different types of rocks and should permit a mix design based on similar proportions of "solids," void-filling, and flow asphalt.

The work involved a literature review on aggregates and various flow models, statistical design of an experiment, laboratory testing, and analysis and comparison of test results with preconceived models and theory. Three different rocks, three rock sizes and three asphalt film thicknesses were represented. Both tension and compression tests at three rates of deformation and at three temperatures were employed.

LITERATURE REVIEW

The literature review included a wide area of particle composites. Only references essential to this paper are

briefly reviewed here, but a more detailed summary can be found elsewhere (1), (2).

Uncoated Aggregates

A number of studies have been made to characterize pieces of rock. The main factors of importance seem to be the following: (a) particle geometry; (b) angularity or roundness; and (c) surface roughness. There are two recent and informative summaries by Gronhaug (3) and Mather (4) based on about two hundred references which discuss the various parameters. The main purpose in the survey was to extract quantitative, descriptive data which can be used in calculations.

In the area of particle geometry, specifically, work by Mackey (5) was helpful in bringing out the concept of ellipsoid as a form best adaptable for the idealization of a shape of an irregular particle.

Roughness has been investigated by a number of authors (6), (7), (8), (9), (10). Bikerman (10) has developed a simple quantitative method for measuring surface roughness of smooth, level areas. He coated flat, sawed rock plates with asphalt, scraped the excess down to the stone, and used the amount of asphalt left as an indicator of surface roughness (and absorption).

Angularity of rock pieces has been determined by several researchers but none of the findings were readily applicable quantitatively. Grønhaug (3) suggests to combine angularity and roughness into one term -- form, but no quantitative

characterization of "form" is given.

In addition to dry particle parameters, literature search for a numerical method of predicting asphalt aggregate behavior from basic ingredients was undertaken. This lead to the so-called contact area model.

Contact Area Model and Theory

The simplest unit in bituminous concrete may be visualized as consisting of two rocks glued together with a drop of asphalt. It is assumed that the two small areas of the rocks facing each other are flat and parallel to each other, and that the asphalt drop between the two rocks will have the shape of a thin cylindrical disc with radius r and thickness h_0. Under these ideal conditions the asphalt acts as an adhesive and the "strength" of this adhesive joint is a function of both the radius and the thickness of the film between the rocks.

This concept leads to the theoretical and experimental work done by Stefan (11). He used a Newtonian liquid between two parallel discs. The mathematical derivation of Stefan's theory has been more clearly presented and interpreted by Bikerman (6), (12) and Majidzadeh and Herrin (13). For two parallel plates or discs having a radius r, with a Newtonian liquid of viscosity η between them and separated by a distance h, the force required to separate the plates at a rate $\frac{dH}{dt}$ is:

$$F = 1.5\eta \frac{V^2}{\pi h^5} \frac{dH}{dt} \qquad (1)$$

where V is the volume of the adhesive material between the plates.

The above theory assumes that a cylindrical plug (or any other shape) of liquid or semiliquid placed between two plates will exhibit flow towards the center of the disc when the plates are separated. The outside edges of the disc will distort in a parabolic fashion and shear forces will develop in addition to tensile forces.

The horizontal flow between two discs occurs because external load creates a pressure difference in the material. If for some reason gas cavities are generated inside the liquid, the above equations are no longer valid. Also, if the rate of deformation is so fast (or temperature so low) that no laminar-shear flow can take place, rupture will occur in tension.

PREDICTIONS AND EXPERIMENTS WITH UNCOATED AGGREGATES

The literature survey indicated that surface roughness and ellipsoid geometry may be useful to characterize individual rock pieces.

The volume of an ellipsoid is:

$$V = \frac{\pi}{6} \ell m s \qquad (2)$$

where ℓ, m, s are the long, medium and short diameters respectively. The volume of a sphere is $\pi/6 \; d^3$ and it can be shown that one-volume spheres and one-volume ellipsoids in cubical and"dense" packing have the same voids (porosities),

namely 0.476 and 0.260.

The equation for surface area of an ellipsoid is rather complicated and a prolate spheroid is often used as an approximation:

$$A = \frac{\pi d}{2} (d - \ell/k \sin^{-1} k) \qquad (3)$$

where

A = surface area of a prolate spheroid

$d = \frac{m+s}{2}$

$k = \left(\frac{\ell^2 - d^2}{2\ell}\right)^{1/2}$

ℓ, m, s = long, medium and short diameters

The surfaces of rocks are not smooth and the asperities of the roughnesses are spaced randomly. Therefore if two pieces of crushed limestone are in contact with each other, the peaks and the valleys will not mesh like two carefully cut gears. Instead, the particles will touch one another at the high spots and only a small portion of the areas will be in contact (14). As a result, the volume which a piece of rock occupies in a mass of other particles encompasses not only the volume of solids and internal voids, but also the volume of the dips and valleys of the particle surface which may be called "outside voids" (Figure 1). These outside voids are primarily a function of the rugosity of the surface. As used in this study, the term "packing volume" when applied to a particle, is that volume which the particle occupies in a mass of particles, or:

$$V_p = V_s + V_i + V_o \qquad (4)$$

where

V_p = packing volume of a particle

V_s = volume of solids of the particle,

V_i = volume of internal voids, and

V_o = volume of outside voids or surface irregularities

The packing volume can be pictured as a volume enclosed by a dimensionless, flexible membrane stretched along the surface of a rock (Figure 1).

In the laboratory, it was proposed to measure packing volume by heating rock and a 55 penetration asphalt to 300° F. (simulating bituminous mix temperature), immersing the heated rock pieces in the heated asphalt for thirty minutes to allow for penetration of surface voids (an attempt to simulate mixing and high temperature storage time), then removing the coated rocks from the asphalt and dipping them into ice water before removal of the excess asphalt coating to achieve a "membrane" condition. After the coated rocks had cooled, they were to be taken out and the excess asphalt removed down to the asperities of the rock piece. As a scraping tool, a razor blade as used by Bikerman (10), was to be tried. Finally, the actual packing volume, V_p, can be obtained by weighing the scraped rock piece in air and water. The rugosity, R, can be simply expressed as the average asphalt film thickness, or $R = V_a/A$ = volume of asphalt after scraping divided by the surface area of the aggregate piece.

The laboratory work involved three types of rocks (crushed limestone, crushed gravel and rounded gravel) with three distinct packing volumes about one decade apart (4 cc, 0.4 cc, and 0.04 cc). The "size" of the rocks was about 3/4, 3/8, and 1/8 inches, respectively (Figure 2). The coefficient of deviation D for each volume group was 15%. The surface rugosity and geometric parameters were measured, packing volumes were calculated, and weights for identical bulk volumes were predicted for the various rocks and sizes. Loose bulk volumes and volumes after vibratory compaction were measured and compared to check the validity of the packing volume approach for one-size dry aggregates.

The three aggregates were selected on the basis of differences in rugosity (crushed versus rounded) and composition (sedimentary versus mixed). These three rock types are frequently used in highway construction. The crushed gravel and the rounded gravel came from the same source. Data on rocks are presented in Table 1.

The rugosity was measured using the previously described method and by making 20 replicates for each point of the curves shown in Figure 3 . As it is seen, rugosity decreases with particle size.

The particle volume distribution of crushed limestone and rounded gravel (or any two aggregates) can be different if taken from the same sieve-size fraction. Figure 4 gives an example of packing volume distribution curves for 1/2 inch to 3/8 inch

crushed limestone and for gravel of the same size. In the case of this limestone and gravel, there is a tendency for the average volume of the limestone particles to be smaller than gravel.

Finally, to check the differences in the shape of ellipsoids, comparisons were made among ℓ/s, ℓ/m, and m/s ratios for various fractions of the rocks, as illustrated in Figure 6.

PREDICTIONS AND EXPERIMENTS WITH MIXES

Prior to laboratory experiments, predictions of mix behavior were made. These were followed by trial experiments, design of the experiment and testing.

Flow Model for a Specimen

The packing volume of a rock includes:

$$V_p = V_s + V_{iv} + V_{ov} \tag{5}$$

where

V_s = volume of solids

V_{iv} = volume of voids impermeable to asphalt

V_{ov} = volume of surface roughness and voids filled with asphalt

Since the asphalt filling the surface voids or the rugosity asphalt is immobilized or stagnant, additional asphalt for lubrication and flow must be added to complete a mix. Here the additional asphalt is called binding or flow asphalt.

When the contact area theory (basically Stefan's theory) is used to predict the flow resistance of a bituminous concrete,

it becomes necessary to make a number of simplifying assumptions (Figure 6). At the beginning, it is assumed that

a. the contact areas between rocks are circular,

b. the two faces of the contact areas are smooth and parallel to each other,

c. the asphalt plug between the two surfaces is cylindrical with radius r and height h_o, where h_o includes the thickness of 2 flow asphalt films,

d. the asphalt is Newtonian.

This simple model provides a good insight for the problem at hand.

Equation (1) for the case of non-immersed round discs was as follows:

$$F = 1.5\eta \frac{V^2}{\pi h^5} \frac{dH}{dt} \qquad (1)$$

This indicates that the film thickness h is of extreme importance with respect to the force F required to pull discs apart or to push them closer together (Figure 6). What Equation (1) does not show clearly is that there is an equally important factor hidden in V^2. This is the radius r of the asphalt plug. It may be best shown by integrating Equation (1) and getting:

$$ft = \frac{3}{8}\eta\left(\frac{r}{h_o}\right)^2 \qquad (6)$$

Here f denotes force per unit area, and h_o is the initial thickness of the asphalt plug. This equation shows that not only is film thickness important, but so is the radius or lateral dimension of the film. In fact, film thickness, according to Stefan's theory, is a relative parameter

because the force "f" or strength of the film per unit area will be identical in such extreme cases as when r = 1 inch and h_o = 1 inch as compared to r = 10 microns and h_o = 10 microns. This important relationship has not been brought out clearly in the literature surveyed and yet it is very helpful when applied to bituminous mixes.

Stefan's equation is basically valid for only one contact plug between two rocks. In a one-size mix there are many contacts, but not all of them will participate to resist tensile or compressive force applied to the specimen.

Cubical packing is the simplest arrangement for spheres or ellipsoids in bulk. In such a case it is easy to calculate the number of rocks M stacked up on top of each other in a given length specimen; also the number of one-size spheres per layer horizontally (L) for a given diameter is simple to calculate. The modified Stefan's equation for a specimen with cubical packing of one-volume spheres:

$$F = \frac{10.73}{10^6}\eta \times \frac{r^4 h_o^2}{(h_o+\Delta h)^5} \times \frac{L}{M} \times \frac{dH}{dt} \qquad (7)$$

where

F = the total force

η = viscosity of asphalt

r = average radius of contact area for the rocks

h_o = average "asphalt" thickness between particles (2 x "film" thickness)

Δh = change in average distance between particles

L = number of rocks -- horizontally

M = number of rocks -- vertically

$\frac{dH}{dt}$ = rate of deformation

The number of contact points for each particle in a cubical packing is 6.

Prediction of Flow Region

From Stefan's theory, using constant rate of deformation:

$$F = g(\eta, r, h) \tag{8}$$

This applies to both tension and compression. Majidzadeh, Marek and Herrin (13), (15) have indicated that for a given asphalt the theory is applicable only over a certain region. In order to gain an insight into what factor is involved in determining the flow and semi-brittle failure regions, Majidzadeh and Herrin's data for one asphalt were used. Calculations for the relative linear strain in the outside "skin" of the asphalt plug, assuming a V-shape neckdown, gave a very interesting and helpful relationship; namely, for the specific 72 penetration asphalt at 77 F, the material between two circular discs deformed and failed by flow when the relative linear rate of strain in the outer "skin" of the plug was below 43 percent per second. This seems to apply to any film thickness used by Majidzadeh and Herrin (13). The final equation for approximate strain in the surface is as follows:

$$\varepsilon = \left\{ \frac{r^2}{h_o^2} \left[9 - \frac{6K^{\frac{1}{2}}}{a+1} + \frac{3K}{(a+1)^2} \right] + (a+1)^2 \right\}^{\frac{1}{2}} \tag{9}$$

where

ε = unit strain in the outer surface

r = radius of the asphalt plug

h_o = thickness of the asphalt plug

a = unit change in h, and

$K = 3(3 + 2a - a^2)$

It is of interest to note here again that the strain is a function of r^2/h_o^2 (plus other factors) just as in Stefan's Equation.

From the derivations above it is apparent that for a given asphalt the line between the flow region and the semi-brittle behavior is a function of (a) temperature, (b) the ratio $(r/h_o)^2$, and (c) the relative rate of widening of gap h_o. Using data from Majidzadeh and Herrin (13), values for Figure 7 were calculated and plotted. This figure separates the flow and intermediate failure regions for this one particular 72 penetration asphalt. Using a tension test similar to Majidzadeh and Herrin's, the flow region can be determined for any asphalt.

Finally, it must be added that Figure 7 can be used for approximate estimates of the flow region for asphalts which are not too different from the 72 penetration asphalt used by Majidzadeh and Herrin, since in most applications the viscosity enters as a first power variable, including Stefan's equation. It was used for estimating the flow region in the experiments with mixes described below.

Choice of Variables

In order to verify the applicability of (a) the packing volume concept with stagnant and flow asphalt, and (b) the

contact area-strength theory, a series of experiments on compacted one-size mixes was performed. Both tension and compression tests were adapted.

In the tension and compression tests, the following variables and coding were used:

Rock type -- rounded gravel, crushed limestone (0,2)

Rock "size" -- 0.04 cc, 0.4 cc, 4 cc (0,1,2)

Asphalt "film" -- 10, 20, 30 microns (0,1,2)

Rate of deformation -- 0.3, 3, 30%/minute (0,1,2)

Temperature -- 60, 80, 100 F (0,1,2)

In the work with uncoated aggregates, rock types used included crushed gravel. However, since the rugosity values of the crushed gravel and crushed limestone were found to be quite similar (Figure 3), only the crushed limestone and the rounded gravel were used in work with mixes.

The three rock volumes of 0.04 cc, 0.4 cc and 4 cc were discussed previously. See Figure 2 and Table 1.

The asphalt film thicknesses chosen were 10, 20 and 30 microns. Film thickness as defined here is obtained by taking the volume of flow asphalt (rugosity asphalt excluded) and dividing it by the total "membrane" area of the rock surface.

Constant rate of deformation instead of constant rate of loading was used to facilitate careful seating of the specimens and to avoid preloading before testing. The actual magnitudes of the rates were selected to be in or near the flow region as defined by Figure 7.

The three temperatures of 60, 80 and 100 F also were selected so as to stay in or near the flow region of the asphalt at the contact points. An attempt was made to go above 100 F , but the one-size mixes were rather weak and were hard to handle without damaging them.

Other variables which were kept constant are discussed in the next section. Altogether six distinct batches of rock were mixed with asphalt. These mixes were prepared by a standardized procedure. Each batch of aggregate had a total packing volume of 565 cc (sum of the packing volumes of individual particles, or ΣV_p).

One 55 penetration asphalt was used in all mixes. Characterizing data on this asphalt are given in Table 2. The asphalt and the aggregate were placed separately in an oven at 280 F and heated for about two hours. Next a precalculated amount of asphalt (Figure 8) was added and mixed by hand in a 2-quart bowl for one minute. The mix was then placed in an unheated (75 F), 12-inch high by 4-inch diameter split mold which was previously lined with a silicone-coated aluminum foil. The specimen was then put on a vibratory table and compacted using a frequency of 20 cps and 1.5 g's maximum acceleration. The standard number of cycles for compaction was 1,000 with one exception which will be discussed later.

The specimens were compacted without a surcharge on the top and therefore levelling and smoothing of the upper surface after vibration was necessary. This was accomplished by 50 light

tampings with a 2-inch diameter, 1,400 gram tamper, dropped each time from a 3/4-inch height. The compacted specimens were almost exactly four inches in diameter and four inches high.

After cooling for two hours at 75 F, the specimens were taken out of the molds. Hard asphalt (15-20 penetration) was used to glue a 3/8 x 4 x 4 inch aluminum plate to each end of the specimen. Then a cardboard jacket was wrapped around the specimen and adjustable spacers were placed at all corners of the plates to keep the specimen from deforming laterally and vertically. The specimen was placed for at least two hours in air at the test temperature.

Specimens were seated and fastened in the same way regardless of the type of test. In other words, the capping and seating was identical in all cases. It follows that the constraints imposed upon the specimens by the plates were similar in all tests.

The electrohydraulic system used for applying the prescribed constant rate of deformation to each specimen consisted of a loading system and a two-channel strip chart recorder; one for recording force, the other for deformation.

There were no essential differences in the method of performing the tension and compression tests, except for the "pull" and "push." The specimens were fastened in a similar manner and all tests were run to at least 2.5 percent axial deformation. This was the highest limit that could be obtained at the slowest rate of deformation with the equipment used.

After testing, the specimens were placed in a solvent (benzene) and the rocks were recovered by cold extraction. These same rocks were used again since the production of a new batch for each specimen would have been very time consuming.

Trial Experiments

As a preliminary step in the experiments with mixes, a 2^5 factorial experiment in tension was performed using the two types of aggregates and the high and low levels of each of the other factors. The results indicated that some of the three-way and perhaps even higher interactions of the factors may be rather large (significant). This was taken into account in the design of the basic experiment.

The same trial experiment also indicated that the rounded gravel mixes had a peak "strength" in tension higher by ten percent or even more than limestone mixes. Since it is known that bituminous mixes in tension are sensitive to void content, the void measurements were compared. The gravel mixes had slightly lower void content for the standard 1000 cycles vibratory compaction. By trial and error it was found that by reducing the compaction to around 100 cycles for the gravel mixes, a void content similar to that of limestone mixes (using 1000-cycle compaction) was obtained. The small differences in strength then disappeared.

Tests in compression showed that the 1000-cycle vibratory compaction gave similar results, as far as force is concerned,

for the two rocks. Thus it was decided to compact the gravel specimens for tension tests for 100 cycles and all others for 1000 cycles. In other words, the tension specimens were made so as to contain equal voids for the comparable gravel and limestone rocks. Compression specimens, on the other hand, all had equal compaction.

Design of the Basic Experiment

As outlined at the beginning of this section, two types of rocks were included in both the tension and compression tests. Since there was no way to describe them numerically, two qualitative levels for rocks were used. The other factors had three quantitative levels each.

The main purpose of the basic experiment was to show that with the help of the packing volume concept and "neutralizing" rugosity, mixes containing gravel and limestone rocks can be made to have similar resistance to flow under a given load. The first goal was to show that the means for "strength" of the mixes containing the two different rocks are the same.

The second goal was to illustrate the effects of other factors. Since it is known that factors like temperature and rate may introduce quadratic terms in descriptive equations, three levels were introduced in the design.

The response variable (y) was the peak force ("strength") for each specimen. In addition, the energy consumed to 2.5 percent axial strain for each specimen was measured and used as a second type of response variable.

If a full 2 x 3 x 3 x 3 x 3 factorial experiment were performed, adding about 15 specimens for replicates, the total number of specimens to be made and tested would have been about 360 for the tension and compression series. To reduce the number of specimens to about 200 , a so-called composite design presented by Box and Wilson (17) was used. The treatment combination for each temperature block can be extracted from Table 3. The design consists of a 2^n factorial plus intermediate points. Analysis of variance can be made on the factorial part and regression analysis on the whole set. The five duplicates in each block were to be used to test whether the higher interactions are large (significant) or small.

The randomization for each type of test over the whole field was impractical because of difficulties with test temperature control. Instead three completely randomized blocks were used, 60, 80 and 100 F . This really is a split plot design.

Force and Energy Comparisons

The results obtained in the tension and compression tests are presented in three ways: first, by selected graphical comparisons, second, by analysis of variance and third, by regression equations.

Graphical Comparisons for Force

Example of force-deformation curves replotted from the strip chart recorder is given in Figure 9. It illustrates the

general similarity in shape and magnitude between curves for specimens made from the two rock types. The maximum force values for tension and compression are tabulated in Table 3. There are six blocks altogether, each containing thirty basic readings plus five replications. The grouping of the data was done in such a way that both analysis of variance (ANOVA) and regression can be made.

Since the comparison between gravel and limestone mixes is so important to the objectives of this study, the average force data for each temperature in tension and compression are presented in Figure 10. These comparisons were obtained by taking one particular temperature in Table 3 and averaging the 15 force values of the "0" rocks (gravel) and 15 values of the "2" rocks (limestone). It is apparent that the gravel and the limestone mixes averaged to be of the same "strength" as suggested by the original hypothesis.

There are a number of ways to make other graphical comparisons of the force values and other variables. Some of them are discussed below.

Figures 11 and 12 show how the force is affected by the highest and the lowest levels of rock size and by film thickness respectively. The average values plotted were obtained by using only the first eight force numbers of each rock type and the three temperatures in Table 3. This gave an average of 24 specimens for each bar graph.

Figures 13 and 14 return to the comparisons between gravel and limestone, but the plots are made using all three levels of each of the variables compared; namely, flow-binder film thickness and particle packing volume.

The general trends in the tension and compression test results appear to be quite similar. There may be some differences in the optimum asphalt film thickness for the two tests (Figure 13). The aggregate size also may affect the maximum force values somewhat differently in the two types of tests (Figure 14). However, more work would have to be done to determine this conclusively.

The most interesting curve in this series is obtained when the average force values for all thirty specimens in each temperature block are compared as shown in Figure 15. The compressive force turns out to be about three times higher than the tensile and the two curves are approximately parallel. This suggests that similar mechanisms are operative within a mix during each type of test.

The values for energy needed to strain a given specimen up to 2.5 percent are listed in Table 4. The tabulation technique is identical to that for force values in Table 3. It should be noted that a strain of 2.5 percent is rather high and, especially in tension, well beyond the so-called failure strain peak force (16). Since the general trends in energy were similar to those of force, no graphical comparisons are shown.

Analysis of Variance (ANOVA)

An example of final ANOVA summary for force at 60 F in tension and for the low and the high levels of the various factors is given in Table 5. The five replicates in each temperature block were used for the estimate of the "pure" error. This, in turn, was applied to check whether some of the higher interactions were too large and should be excluded from the error term. Using the F test and a 5 percent significance level, in practically all cases some of the 3-way interactions were found to be unacceptable for use in the error term. These interactions were taken out of the computations of the final F test values, but they may be real. In the interest of brevity the remaining ANOVA tables are not included.

The analysis of variance shows that there is no significant difference in the average peak force, both in tension and compression for specimens made from the two rock types.

The ANOVA also shows that the size of the rocks (4 cc versus 0.04 cc) and the rate of deformation (30%/min. versus 0.3%/min.) produced highly significant differences in the force and energy values, while an increase in the flow asphalt from 20 microns to 60 microns produced less significant differences.

Regression Analysis

The analysis of variance was performed using only the high and low levels of the factors in each of the six

temperature blocks. Since all of the factors except the rock type had three quantitative levels each, a regression equation for the force and energy values could be constructed. This was done using a computer and a stepwise regression program in which only the significant variables or combinations thereof are retained in the operation. The equations for force in compression and tension follow. The whole plot error was negligible:

$$y_t = 37.37x_1+11.23x_2+29.58x_3-2.427x_4+3.240x_{11}-0.03756x_{22}-2.678x_{12}-0.1300x_{33}-3.592x_{13}-0.08039x_{23}+0.02353x_{123}+0.02706x_{44}-0.6200x_{14}-0.1169x_{24}+0.03211x_{124}-0.2768x_{34}+0.04058x_{134}+0.00146x_{234}-0.00040x_{1234}+\text{error} \quad (11)$$

$$y_c = 17.63x_1+36.56x_2+92.82x_3-6.480x_4+26.79x_{11}-0.1935x_{22}-7.793x_{12}-0.6456x_{33}-10.25x_{13}-0.7567x_{23}+0.2697x_{123}+0.07064x_{44}-1.624x_{14}-0.3494x_{24}+0.09450x_{124}-0.7973x_{34}+0.1180x_{134}+0.01030x_{234}-0.00343x_{1234}+\text{error} \quad (12)$$

where

y_t = peak tensile force on specimen, in pounds

y_c = peak compressive force on specimen, in pounds

x_1 = packing volume of rock in cc's

x_2 = asphalt film thickness, in microns

x_3 = rate of deformation, in percent per minute, and

x_4 = test temperature in F.

Strain at Peak Force

The strain applied to a specimen when the maximum force is reached was obtained from the data curves for the tension and compression tests. The numerical average values are given in Figure 16. As can be seen, the amount of strain at peak load in both tension and compression is about the same for both rounded gravel and crushed limestone mixes, especially at higher temperatures where flow deformation (no brittleness) is predominant.

It is of interest to note that the peak load strain in tension is close to 1/2 percent, regardless of the temperature. This agrees closely with published literature on a typical graded dense surface mix (16).

In compression the peak load strain was about three times higher than in tension or similar to the relationship between the peak force in the two tests. The temperatures used in this experiment do not seem to cause differences in the "failure" strain values in compression.

Analysis Using Contact Area Theory

The results discussed so far were aimed primarily at proving that two mixes composed of different rocks, graded by packing volumes, can be made to have similar flow properties by neutralizing the rugosity of a rock and then adding

a prescribed amount of binding or active asphalt. The next question is whether there is a way to predict the actual flow resistance of the mixes once the rugosity has been accounted for and the amount of binding asphalt, plus other measurable parameters, is known.

Such a prediction was attempted using Stefan's theory. The basic equation is:

$$F = \frac{10.73\eta}{10^6} \times \frac{r^4 h_o^2}{(h_o + \Delta h)^5} \times \frac{L}{M} \times \frac{dH}{dt} \qquad (13)$$

where all symbols are as previously shown. They are also discussed individually in the sections below. It must be repeated that the use of this equation presupposes a simple and idealized model with a number of assumptions. Nevertheless, agreement between the test results and the predicted values in the flow region is quite encouraging, especially in tension.

Tension Test Analysis

The values for variables used in Equation (13) are summarized in Table 2 and the Appendix, including one example of the calculations. Example of graphical comparisons between the predicted and experimental values of peak force is shown in Figure 17. The viscosity values are given in Table 2. Since it was not easy to define the actual shear rates encountered at the contact points of the rocks, and since the main interest was in the flow region at 100 F and 80 F, it was assumed that the asphalt exhibited Newtonian flow.

Therefore a single value of viscosity for each temperature was used in the calculations.

The contact radius "r" was measured in the laboratory. This was accomplished by taking a compacted mix apart and selecting rocks at random. By means of a magnifying glass and a ruler the approximate radii of contact points were measured to the nearest 0.01 inch. It was apparent that the size of "r" varied and a distribution of "r" rather than a single value was obtained. The average "r" was used in the calculations (Appendix).

For the h_o, the value of two times the flow film thickness was used. It was assumed that there is an asphalt plug of average thickness of h_o and radius "r" between the contacts of two rocks. This further implies that the surfaces of the two rocks at the contact points are flat and parallel to each other.

The value Δh was calculated by taking the total axial strain in the 4-inch long specimen and dividing this by the number of estimated contact points in tension along the axis of the cylinder. The packing of the rocks was assumed to be cubical.

Figure 17, lower part, shows that one of the best agreements with theory is found with the small rocks, at high temperature, with thick asphalt films and at the slow rate of deformation. This falls into the flow region where apparently even in mixes with irregular contact surfaces the asphalt

exhibits mainly flow and necking behavior as in the case of thick films between plates described by Majidzadeh, Marek and Herrin (13), (15).

Since certain simplifying assumptions are involved, it cannot be expected that the theory and the results would always agree as closely as in the lower part of Figure 17. Perhaps a two or three magnitude difference between predicted and actual results is acceptable under the circumstances.

In general, it can be said that there is more difference between the measured and the predicted values for force as the "size" of the rocks increases. Most likely this is due to the fact that the asphalt plug between any two rocks is defined numerically not only by the thickness or height but also by the radius of the contact. Thus for the same film thickness the radius "r" will be greater for a larger rock than for a smaller one. Consequently the film will flow with more difficulty and there might even be cohesive failure within the asphalt (formation of bubbles and strings) thus reducing the actual test strength compared to the theoretical prediction.

Finally, it should be recalled that Newtonian behavior of the asphalt was assumed for all temperatures and rates. This may be satisfactory for 100 F and 80 F and at the slower rates of deformation, but the 60 F region and faster rates are probably not very accurately represented by this assumption.

Compression Test Analysis

The application of Stefan's theory to the compression data presented a more difficult problem than the tension data. In the first place, the strain at the peak compressive force was around 1 1/2 percent (Figure 16) and it is inconceivable for a 20-micron asphalt thickness (h_o) at the contacts of a large-rock specimen to be compressed by such a large amount. Some other mechanism besides compression or squeezing of the asphalt plug outwards from the initial contact area must be taking place. The compressive test data obtained in the laboratory were compared with two values: (a) the theoretical compressive strength using the simple model as in tension with average contact asphalt thicknesses of 20, 40, and 60 microns (h_o); and (b) a shear model with the same values.

In order to set the minimum possible value for compression the increment Δh in the compression model was assumed to be zero and the force was reduced to:

$$F_c = \frac{10.73}{10^6} \times \eta \times \frac{r^4}{h_o^3} \times \frac{L}{M} \times \frac{dH}{dt} \qquad (14)$$

The shear resistance values were calculated by the formula:

$$F_s = \frac{2.248}{10^6} \times \eta \times \frac{dx}{dh_o} \qquad (15)$$

where

F_s = shear force in pounds

η = viscosity of asphalt in poises, and

$\frac{dx}{dh_o}$ = shear rate in sec^{-1}

The sliding plane was assumed to be at 45^o.

Calculations for shear force and compressive force were carried through for all combinations of variables and sample computations are given in the Appendix. The calculated or theoretical values were compared graphically with the experimental results. Examples are shown by Figures 18 and 19. The various comparisons indicated that only for the smallest rocks and the 30-micron asphalt film is the theoretical curve anywhere close to the experimental one, while the calculated shear resistance values are much closer to the experimental. The comparisons suggest that there is little if any compression and squeezing of the asphalt plug between two rocks during the compression test and that the deformation is mainly due to shear flow. In other words, the compressive force as predicted by the Stefan equation is larger than that predicted by the sliding shear force equation. Therefore shear governs the mode of failure.

The predicted shear values can be divided into three categories: a) below the laboratory test values; b) about equal; c) higher than the laboratory test values. The curves of Figure 20 are presented to illustrate the three areas.

When predicted values are below the measured results, this may be due to the pure shear resistance of the asphalt being augmented by direct particle-to-particle contact and friction. This contact can easily occur at high temperatures (100 F) when the asphalt is "soft" and also if the test is run very slowly (Area 1, Figure 20).

The other extreme takes place when the temperature is low (60 F), the asphalt films are thin, and they are sheared at a fast rate. Due to stress concentrations the film is disrupted. The result is a lower shear force in the experiment than the prediction from theoretical calculations (Area 3, Figure 20).

Between these two extremes there is an area of close agreement between the experimental and the theoretical values. These results probably represent pure shear response of the asphalt plug alone.

If the above explanations are applied to the ninety specimens tested, most of the predictions look satisfactory.

Tension and Compression Compared

One of the most interesting findings is the approximate relationship between tensile and compressive peak force:

$$3 F_{P\ \text{tension}} \approx F_{P\ \text{compression}} \qquad (16)$$

as illustrated in Figure 15. Various justifications are possible. First, it is known that many materials have a similar numerical relationship between tensile and shear force.

A more rigorous explanation is suggested by the behavior of a specimen tested well within the region of pure flow -- one with small aggregate, high asphalt content tested at a slow rate of deformation. If the predicted theoretical shear curve is plotted and compared with a similar predicted theoretical tension curve, as is done in Figure 21, the two differ by a factor of approximately two to three, just as in the experimental results.

SUMMARY AND APPLICATIONS

The results obtained in the laboratory work collaborated with the theoretically predicted trends. Thus it is thought that one approach for a unified physical characterization of aggregate and binder composites to predict and explain their behavior has proven successful so far. Although additional work with one-size and graded aggregates is needed, there are certain findings which are useful and applicable currently:

The work has indicated that mixes of similar "strength" can be made with both round, smooth gravel and crushed limestone provided that the aggregates are graded according to packing volume and the amount of binding asphalt is the same. The additional asphalt for filling surface voids is varied depending on the surface roughness of the rock. This investigation included aggregate "sizes" between 0.04 cc and 4 cc or approximately 1/8 to 3/4 inches.

The findings show quantitatively how the amount of rugosity asphalt changes considerably with aggregate packing volume (size) and how a simple aggregate surface area approach for estimating asphalt contents is not applicable, especially for crushed particles.

In the flow region bituminous films apparently fail in shear, under both tensile and compressive forces. This opens new, untried approaches for changing the properties of these films to improve both compressive and tensile strength at the same time.

CONCLUSIONS

The conclusions are based on theoretical considerations and laboratory work with certain crushed limestone, crushed gravel and rounded gravel aggregates of three packing volumes; namely, 0.04, 0.4, and 4 cc (about 1/8, 3/8 and 3/4 inch respectively) with and without asphalt. Although several important aggregate and mix variables have been included on a fairly broad scale, it is probable that these conclusions can be applied to a wider range of aggregates and mixes than those studied. Strictly speaking, the extension of the validity of the findings beyond the specific scope of this study remains to be demonstrated.

1. Particle packing volume, the volume which a piece of aggregate occupies in a mass of other particles, is a parameter unifying the bulk behavior of coarse aggregates.

2. The packing volume of a particle is a function of the volumes of solids, internal voids, and surface roughness or rugosity of the rock piece.

3. The rugosity volume of a rock is a function of, (a) "surface area", and (b) roughness of the rock surface. The area and the roughness vary with rock size, but in opposite directions.

4. When asphalt is added to aggregates, a certain amount of it is used to fill up the surface voids or the rugosity volume, and does not participate in flow when load is applied. This is called rugosity asphalt or stagnant asphalt and its addition completes the packing volume of each rock piece.

5. If a flow or binding asphalt is introduced in addition to the rugosity asphalt, a unified approach to mix design may be possible using different types of aggregates.

6. With the help of Stefan's theory (hydro-dynamic theory), the expected peak force for a compacted specimen can be closely predicted in or near the flow region when the flow asphalt alone is considered as the "working" asphalt.

7. Two geometric parameters which affect the "strength" of a mix are, (a) average radius of asphalt contact "plug" between rocks, and (b) the thickness of the plug or film thickness. The ratio of radius/film thickness is important, rather than the film thickness alone.

8. If the rate of strain imposed in the "necked down" surface of an asphalt plug between two rocks exceeds a certain critical limit, the asphalt plug will "fail" in cohesion (hole forming and stringing) instead of flow and "necking".

ACKNOWLEDGEMENTS

The authors wish to acknowledge the assistance of the Bureau of Public Roads, U. S. Department of Commerce, who supported the investigation with the Indiana State Highway Commission.

Laboratory testing and experimental techniques were carried out in the Bituminous Materials Laboratory of the Joint Highway Research Project at Purdue University, Lafayette, Indiana.

BIBLIOGRAPHY

1. Tons, E. "Flow in Aggregate-Binder Mixes," Ph.D. Thesis, Purdue University, June 1969.

2. Tons, E. and Goetz, W. H., "Packing Volume Concept for Aggregates," Highway Research Record Number 236, Highway Research Board, 1968.

3. Gronhaug, A. "Evaluation and Influence of Aggregate Particle Shape and Form." Statens Vegvesen Veglabaratoriet, Oslo, Meddelese Nr. 31, Oslo, 1967.

4. Mather, Bryant. "Shape, Surface Texture and Coatings of Aggregates." U.S. Army Engineer Waterways Experiment Station, Corps of Engineers, Vicksburg, Mississippi, Miscellaneous Paper No. 6-710, 1965.

5. Mackey, R. D. "The Measurement of Particle Shape." Civil Engineering and Public Works, Vol. 60, No. 703, pp. 211-214, 1965.

6. Bikerman, J. J. The Science of Adhesive Joints. Academic Press, 1961.

7. Broadston, J. A. "Surface Finish Measurement Instrumentation," April and June, 1959.

8. Mikelston, W. "Surface Roughness Measurements of Inspection," Conference of Instrument Society of America, Pittsburgh, Pennsylvania, 1946.

9. Herschmann, H. K. Technical News Bulletin. National Bureau of Standards, Vol. 31, No. 3, March 29, 1947.

10. Bikerman, J. J. "Adhesion of Asphalt to Stone." Massachusetts Institute of Technology, Civil Engineering, Research Report R 64-3, 1964.

11. Stefan, J., (In German), Sitzberichte Kaiserl, Akad., Wiss. Wien, Math - Naturw Klasse, Abt. 2, 69, 713 (1874).

12. Bikerman, J. J. "The Fundamentals of Tackiness and Adhesion," Journal of Colloidal Science, Vol. 2, pp. 163-175 (1947).

13. Majidzadeh, K., and Herrin, M. "Methods of Failure and Strength of Asphalt Films Subjected to Tensile Stresses," Highway Research Board, Highway Research Record No. 67, Publication 1251, pp. 98, 1965.

14. Adamson, A. W. Physical Chemistry of Surfaces. Interscience Publishers, Third Printing, 1964.

15. Marek, C. R. and Herrin, M. "Tensile Behavior and Failure Characteristics of Asphalt Cements in Thin Film," University of Illinois, Private Communication, 1968.

16. Tons, E. and Krokosky, E. M. "Tensile Properties of Dense Graded Bituminous Concrete," Proceedings, Association of Asphalt Paving Technologists, Vol. 32, pp. 497, 1963.

17. Box, G. E. P. and Wilson, K. B. "On Experimental Attainment of Optimum Conditions," J. Royal Stat. Soc. B., Vol. 13, pp. 1-45, 1951.

TABLE 1

DATA ON AGGREGATES

	Rounded Gravel			Crushed Gravel			Crushed Limestone		
	0.04	0.4	4cc	0.04	0.4	4cc	0.04	0.4	4cc
Approximate Size, inches	1/8	3/8	3/4	1/8	3/8	3/4	1/8	3/8	3/4
Average Packing Volume, cc	3.71	0.297	0.041	3.61	0.291	0.039	3.66	0.252	0.036
Rugosity, cm	0.0026	0.0034	0.0044	0.0080	0.017	0.027	0.0077	0.016	0.025
Apparent Specific Gravity	2/67	2/67	2/67	2/67	2/67	2/67	2.71	2.71	2.71
Bulk Specific Gravity	2.54	2.54	2.54	2.54	2.54	2.54	2.66	2.66	2.66
Average Particle S.A., cm^2	0.61	2.31	12.6	0.60	2.45	12.1	0.58	2.40	12.4

TABLE 2

DATA ON ASPHALT

Viscosity at 60 F, 0.05 sec^{-1} Shear Rate, Poises	4.4×10^7
Viscosity at 80 F, 0.05 sec^{-1} Shear Rate, Poises	2.0×10^6
Viscosity at 100 F, 0.05 sec^{-1} Shear Rate, Poises	1.7×10^5
Penetration at 77 F, 100 g., 5 sec.	55
Softening Point, R & B, F	121
Ductility at 77 F, cm	100+

TABLE 3

FORCE IN POUNDS FOR SPECIMENS
IN BASIC EXPERIMENT

Specimen	Tension			Compression		
	60 F	80 F	100 F	60 F	80 F	100 F
0000	23(25)*	1.7	.3	74	9	.7
0200	11	.4(1.0)	.1	23	3	.3
0020	21	1.7	.2(.2)	78	7.5	.4
0220	9	1.1	.1	32	4.4	.4
0002	300	50	14 (16)	750	95	50
0202	160	33	4.0	500	83	13
0022	365	73	17	910	140	56
0222	160	35	9	585	90	24
0111	76	11	2.0	190	37	6.2
0211	26	5.2(7.0)	1.0	89	13	4.3
0011	75	11	2.5	312	30	9 (7)
0121	78	8	1.7(2.0)	220	35(24)	8.5
0101	65(80)	10	1.0	245	30	5
0112	250	50(55)	14	550(545)	145(125)	46
0110	19	1.8	.2	50	7.5	.5(.6)
2000	18	1.0	.2	72(68)	9	.7
2200	12	.8	.1	25	3	.3
2020	17	1.5	.2	92(73)	7.5	.5
2220	10	.9	.1	25	3 (4)	.3
2002	270(325)	53(50)	13	850	100	54 (65)
2202	165(150)	31(29)	5.0	505	80(95)	14
2022	375	70	15	940	205(230)	70 (68)
2222	160	32	6.0(5.0)	460(440)	82	20 (23)
2111	75	9	1.8	193	33	6.3
2211	35	5.4	1.0	145	17	4.5
2011	68	9	2.5	377	27	9.5
2121	65(70)	6	1.5	230(190)	33	5.5(6.0)
2101	60	9	1.5	230	28	6.2
2112	285	47	11 (10)	700	155	46
2110	16	2.0	.2	50	5.5	.5

*replicates

TABLE 4

ENERGY IN INCH-POUNDS x 100

FOR BASIC SPECIMENS STRAINED TO 2.5%

Specimen	Tension			Compression		
	60 F	80 F	100 F	60 F	80 F	100 F
0000	198(198)*	10	.4	650	78	4.4
0200	76	2(4)	.2	180	27	2
0200	192	14	.4(.6)	660	68	4.8
0220	44	6	.2	280	38	2.8
0002	2500	390	112	5700	760	356
0202	770	176	88(116)	3850	700	106
0022	3250	650	132	5900	1480(1580)	416
0222	1140	200	48	4950	780	204
0111	630	100	16	1460	286	48
0211	200	40(46)	6	830	156	36
0011	640	98	22	2540	192(210)	78(44)
0121	670(720)	68	14(18)	1940	296	70
0101	530	78	12	2100	262	46
0112	1850	420(470)	118	4600	1160(1100)	372
0110	168	12	.4	450(400)	50	4.4
2000	160	6	.4	600(520)	74	5.6
2200	102	4	.2	230	30	2
2020	152	13	.4	720(600)	64	4.8
2220	90	6	.2	230	28(34)	2.4
2002	2350(2650)	390(430)	112	5900	760	380
2202	1460(1480)	246(260)	88	3950	660(710)	84
2022	3200	640	132	5400	1475	455(400)
2222	1420	276	48(44)	3750(3050)	630	156(148)
2111	700	86	16	1320	286	40
2211	300	40	6	1110	156	36
2011	610	84	21	2540	192	76
2121	600(800)	50	14	1600(1240)	296	40(42)
2101	550	70	12	1940	262	46
2112	2400	420	100(94)	4500	1160	340
2110	140	16	.4	400	50	4

*replicates

TABLE 5

ANOVA FOR FORCE AT 60 F, TENSION

Source	df	MS	F
A (Rocks)	1	30	.35
B (Rock Size)	1	30800	366.67*
A x B	1	81	.96
C (Asphalt Cont.)	1	1560	18.57*
A x C	1	81	.96
B x C	1	1936	23.04*
A x B x C	1	132	--
D (Rate of Def.)	1	210222	2502.64*
A x D	1	4	.04
B x D	1	24646	293.40*
A x B x D	1	12	--
C x D	1	1849	22.01*
A x C x D	1	72	--
B x C x D	1	1892	--
A x B x C x D	1	121	--

Pure error using 5 replications

$$\text{pure} = 208$$

BCD - significant at the 5% level

Using 4 remaining higher interactions for error:

$$= 84 \text{ with } 4 \text{ df}$$

$$F_{1,4(.95)} = 7.71$$

* Significant at the 5% level.

TABLE 6

PERCENT AIR VOIDS IN EACH SPECIMEN

Specimen	Compression			Tension		
	60 F	80 F	100 F	60 F	80 F	100 F
0000	30.7	30.7	30.7	33.2	33.2	32.8
0200	32.2	32.2	32.9	35.3	33.5	34.7
0020	28.8	28.8	28.1	32.1	30.1	30.1
0220	29.7	30.4	31.1	33.0	32.3	32.3
0002	30.7	32.6	30.7	32.0	33.9	32.0
0202	31.6	30.2	30.2	33.5	33.5	34.1
0022	29.7	28.1	29.5	30.1	32.1	30.1
0222	31.1	31.1	30.4	33.0	30.4	33.0
0111	32.6	32.0	32.0	30.7	32.7	33.2
0211	30.8	28.7	30.8	33.2	32.6	30.8
0011	29.6	32.9	30.3	32.9	32.2	30.9
0121	31.3	32.0	32.0	33.2	33.2	31.3
0101	32.5	31.9	31.9	33.8	34.4	33.8
0112	32.6	32.0	32.0	33.3	32.7	32.6
0110	32.6	32.0	32.6	33.9	33.3	33.3
2000	32.0	32.0	32.0	33.2	32.7	32.0
2200	33.5	33.5	32.9	32.9	33.5	33.5
2020	30.4	29.8	30.4	31.1	29.8	29.8
2220	33.0	32.3	33.6	33.0	32.3	32.3
2002	32.7	32.7	32.0	32.6	32.6	32.0
2202	33.5	33.5	33.5	33.5	32.9	32.9
2022	30.4	31.1	30.4	29.1	28.5	29.8
2222	32.7	34.8	32.7	33.6	33.6	31.7
2111	32.4	32.4	31.9	31.9	31.9	31.1
2211	34.5	30.8	30.8	33.9	34.5	30.8
2011	30.3	31.6	30.9	32.2	31.6	30.3
2121	31.2	31.8	31.8	32.5	32.5	29.9
2101	31.1	31.8	31.1	33.1	33.1	32.4
2112	31.1	31.9	31.9	31.9	31.9	30.0
2110	32.4	31.1	31.9	32.4	30.0	30.0

TABLE 7

PERCENT STRAIN AT PEAK LOAD
TO THE NEAREST 0.25%

Specimen	Compression			Tension		
	60 F	80 F	100F	60 F	80 F	100 F
0000	2	1.5	1	.5	.25	.25
0200	1	1.5	1	.25	.25	.25
0020	2.5	1.5	1	.75	.5	.25
0220	1	1.5	.5	.25	.75	.5
0002	2.5	2.5	2.5	.75	.25	.25
0202	1	1	2.5	.25	.5	.5
0022	2.5	2.5	2.5	1.0	.25	.25
0222	1.5	1	.5	.5	.5	.25
0111	2.5	2	2	.5	.5	.25
0211	1	1	2.5	.5	.5	.25
0011	2	2	2	.75	.25	.25
0121	2	2	2	.5	.25	.25
0101	2	1.5	1.5	.5	.25	.25
0112	2.5	2	2.5	.75	.25	.5
0110	2	1.5	2	.5	.25	.25
2000	2.5	1.5	2	.5	.25	.25
2200	1	1.5	1	.25	.25	.25
2020	2.5	1.5	1	.5	.5	.25
2220	1	1	.5	.5	.25	.5
2002	2.5	2.5	2.5	1.0	.25	.5
2202	2.5	2	2.5	.75	.5	.5
2022	2.5	2.5	2.5	1.0	.75	.25
2222	1.5	1.5	.5	.75	.5	.25
2111	2.5	2.5	2.5	.75	.5	.25
2211	2	1	2.5	.75	.25	.25
2011	2	2.5	2	.75	.25	.25
2121	2.5	2	2	.75	.25	.25
2101	2.5	1.5	2.5	.75	.5	.25
2112	2.5	2.5	2.5	1.0	.75	.5
2110	2	1.5	2	.5	.25	.25

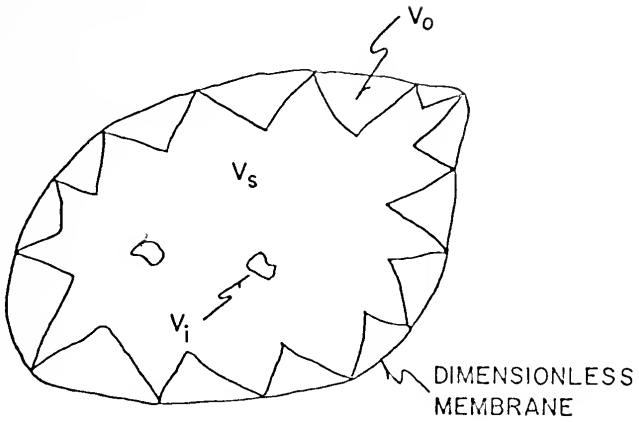

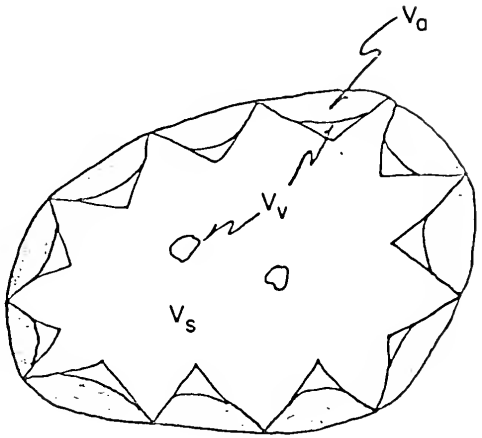

THEORETICAL

$$V_p = V_s + V_i + V_o$$

PRACTICAL

$$V_p = V_s + V_v + V_a$$

FIGURE 1 COMPONENTS OF A PARTICLE PACKING VOLUME

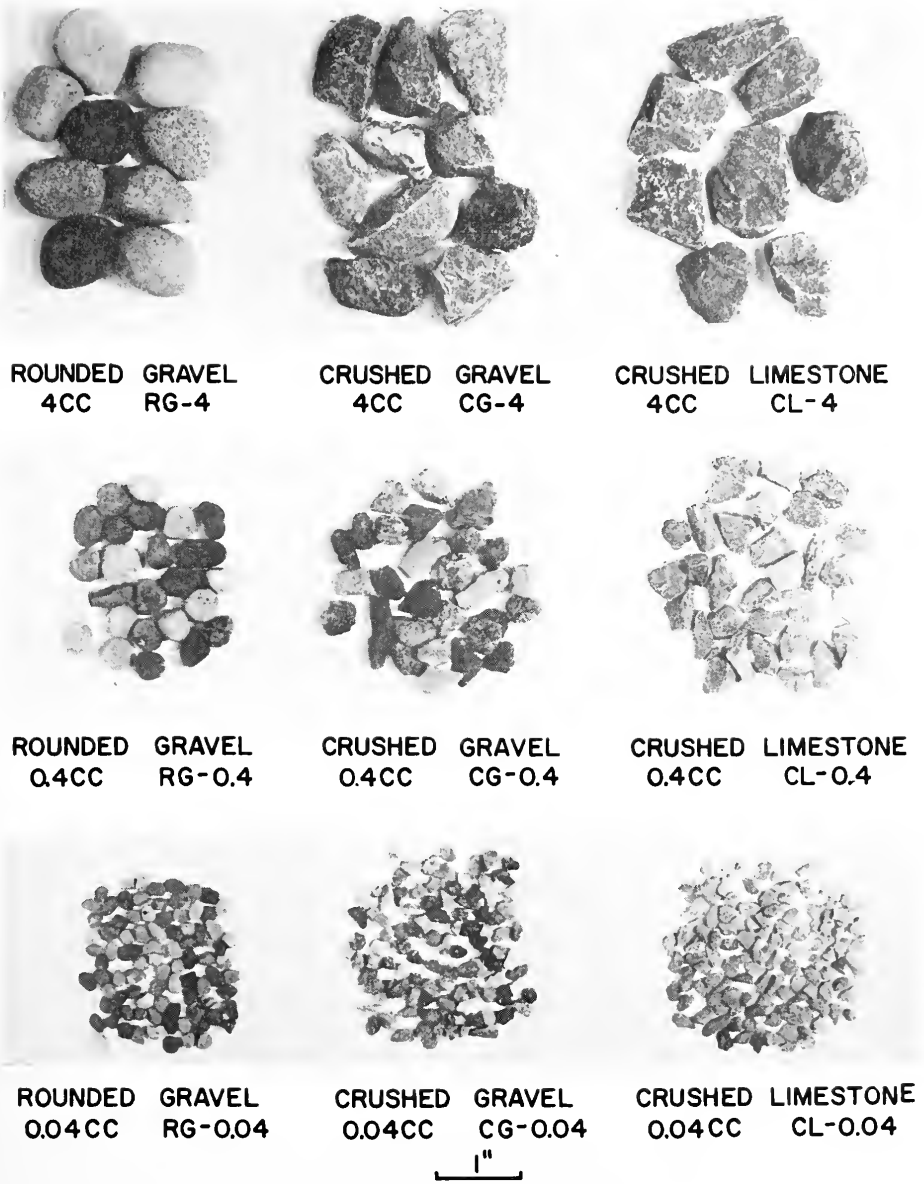

FIGURE 2 TYPES AND SIZES OF ROCKS USED IN THIS STUDY

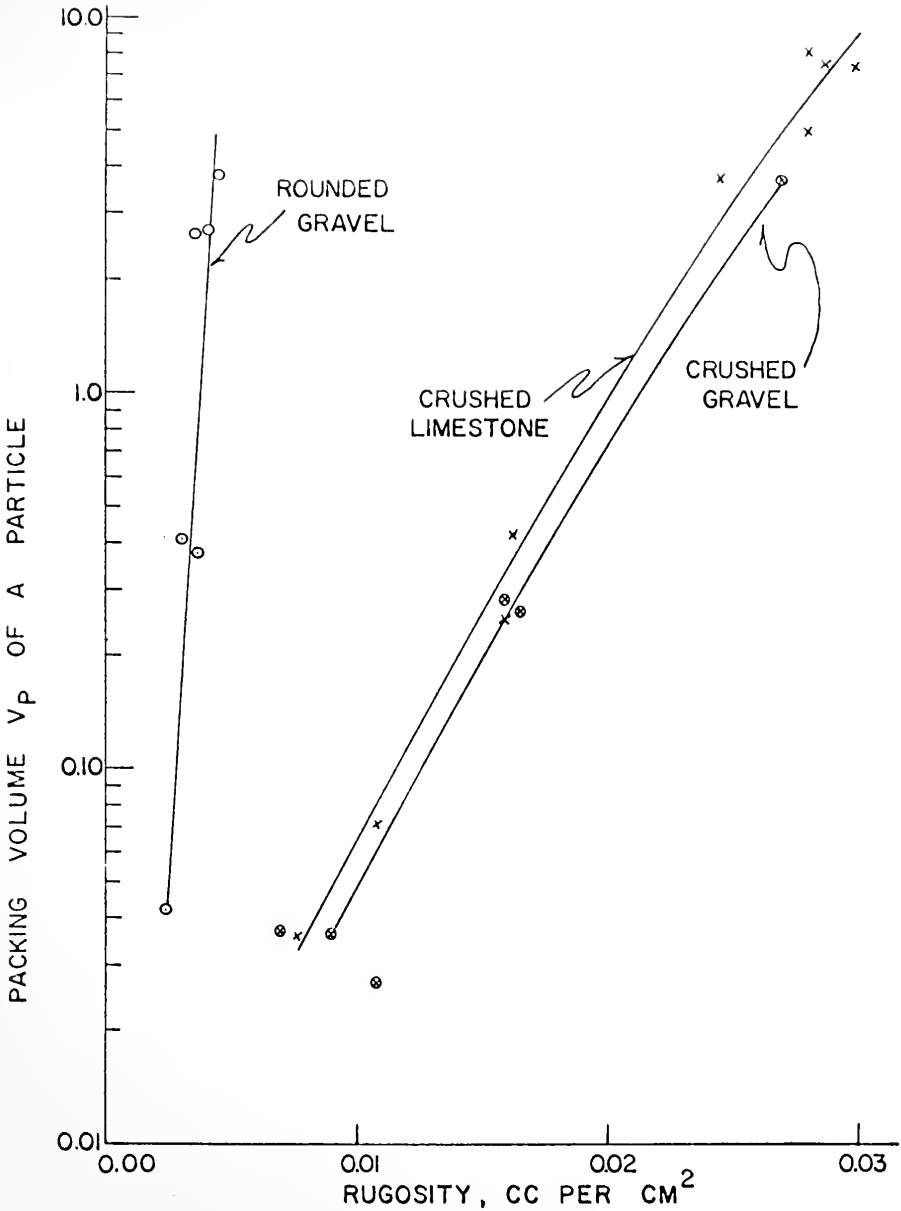

FIGURE 3 RUGOSITY VERSUS PACKING VOLUME FOR THE THREE TYPES OF ROCKS

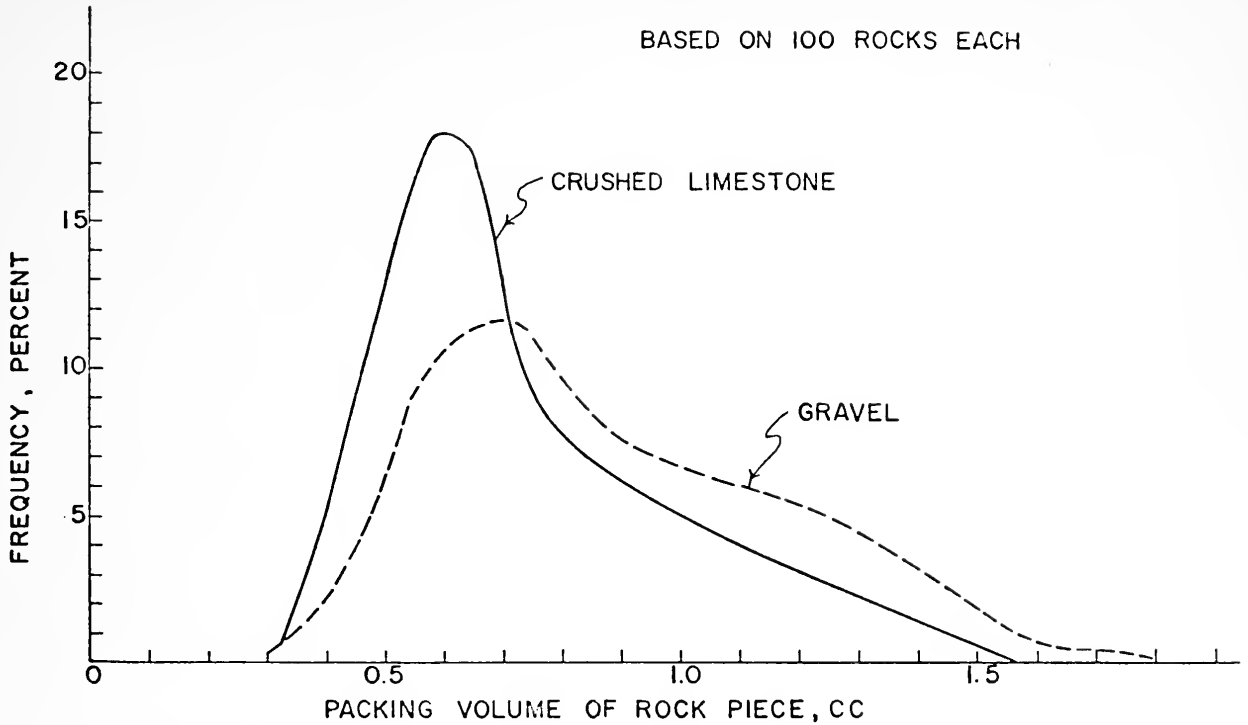

FIGURE 4 EXAMPLE OF PARTICLE VOLUME DISTRIBUTION FOR 1/2"–3/8" CRUSHED LIMESTONE AND PARTIALLY CRUSHED (ABOUT 50% PARTICLES) GRAVEL.

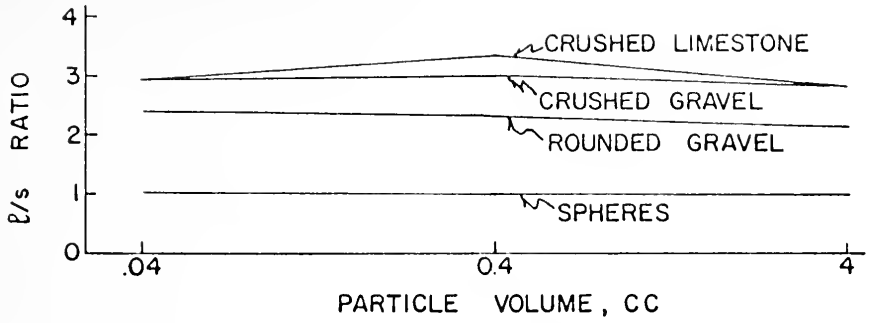

FIGURE 5 RATIO ℓ/s FOR VARIOUS AGGREGATES

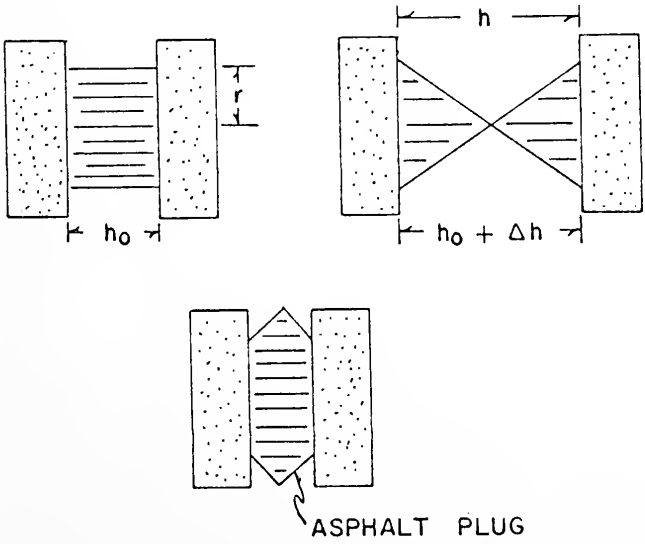

FIGURE 6 DISTORTION OF IDEALIZED CYLINDRICAL ASPHALT PLUG

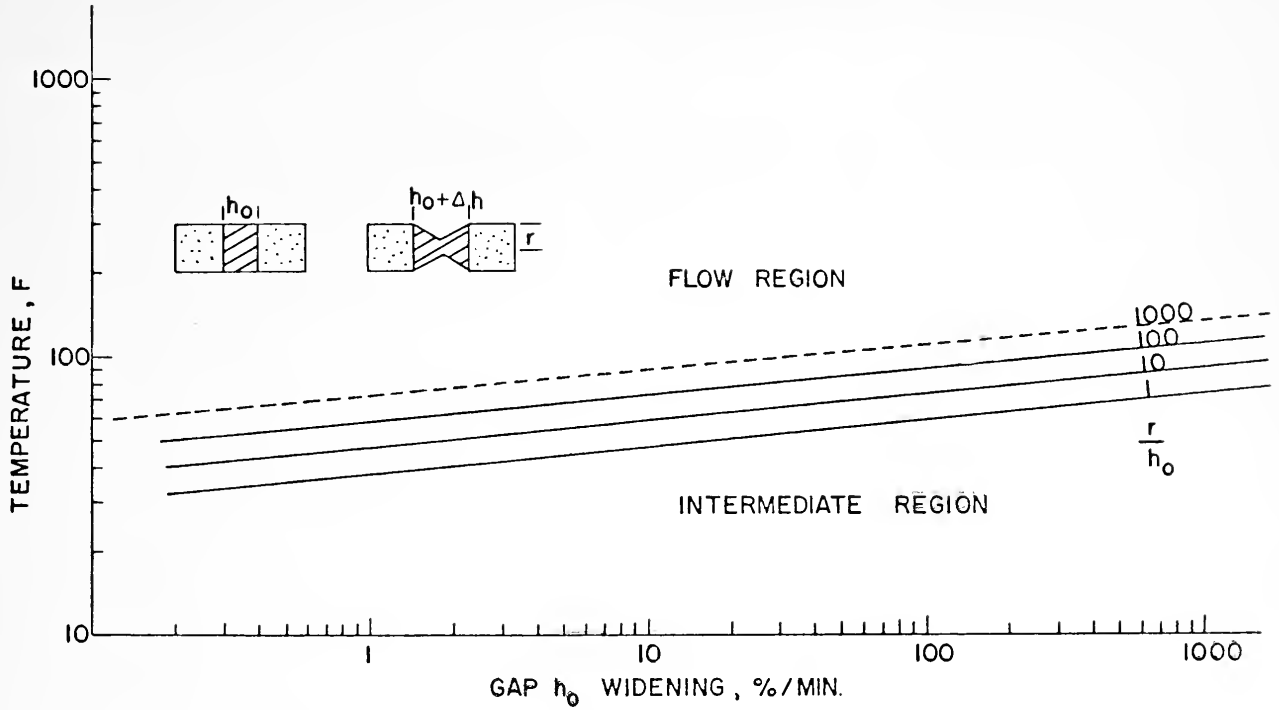

FIGURE 7 MAXIMUM RATE OF LINEAR GAP WIDENING FOR FLOW CONDITION, 72 PEN ASPHALT, USING MAJIDZADEH'S DATA

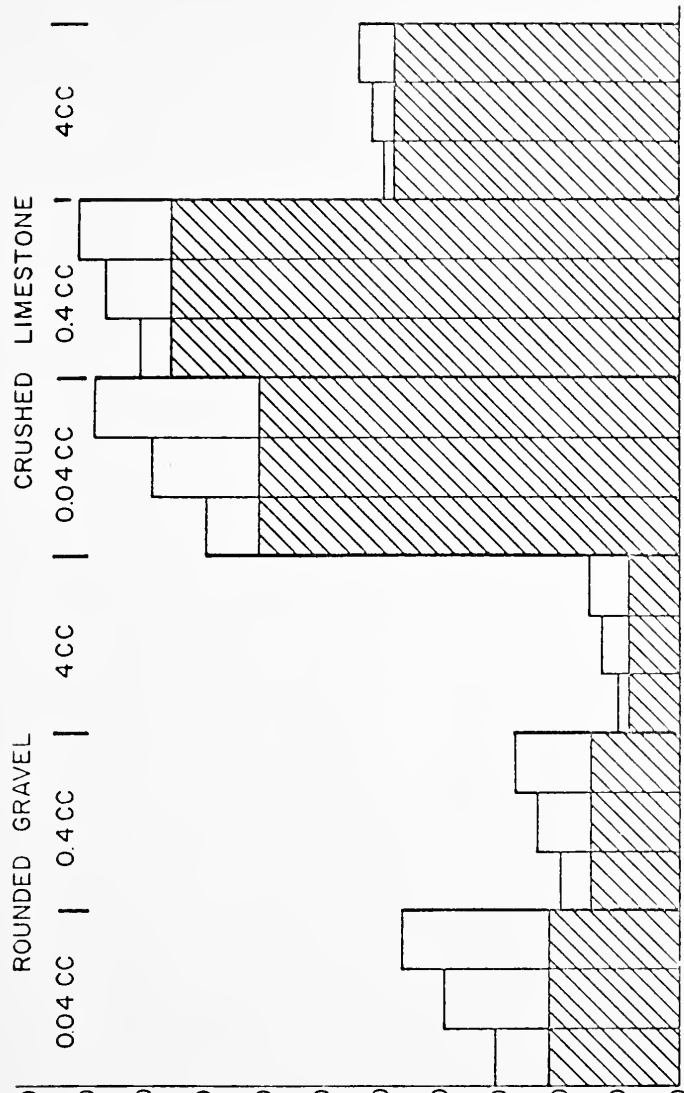

FIGURE 8 TOTAL ASPHALT IN EACH SPECIMEN (GRAMS) FOR VARIED FILM THICKNESS.

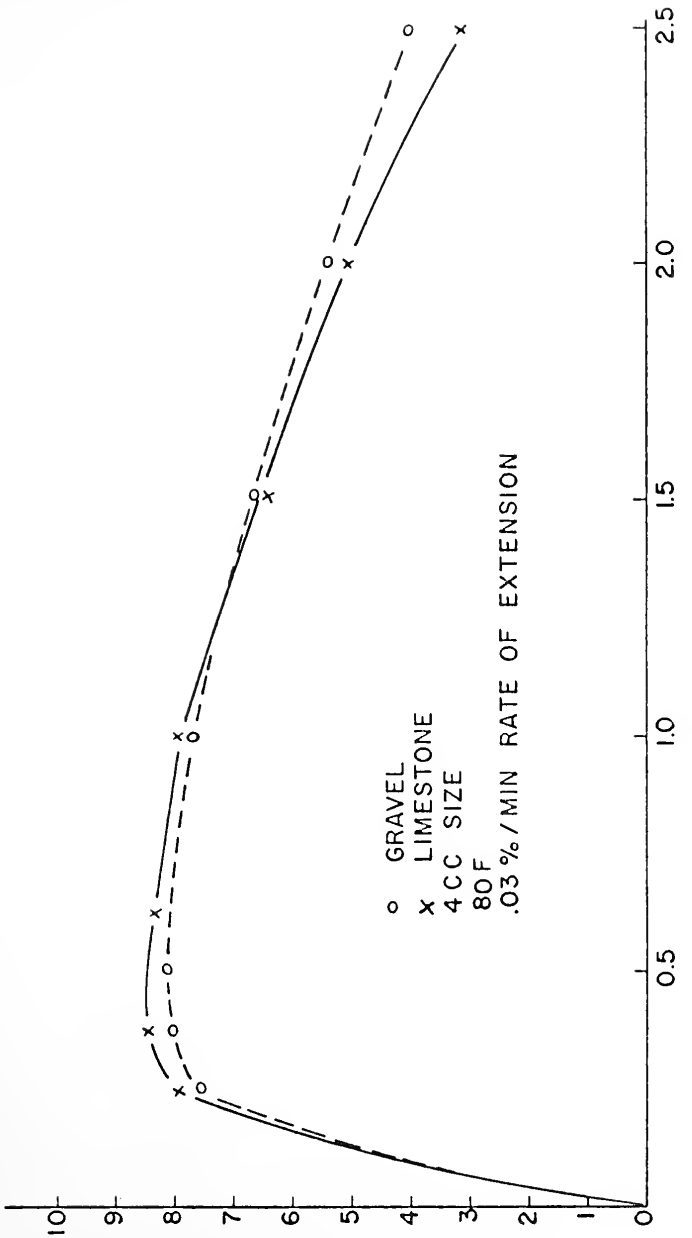

FIGURE 9 FORCE–DEFORMATION CURVES FOR COMPARABLE GRAVEL AND LIMESTONE SPECIMENS, IN TENSION, 4CC ROCKS

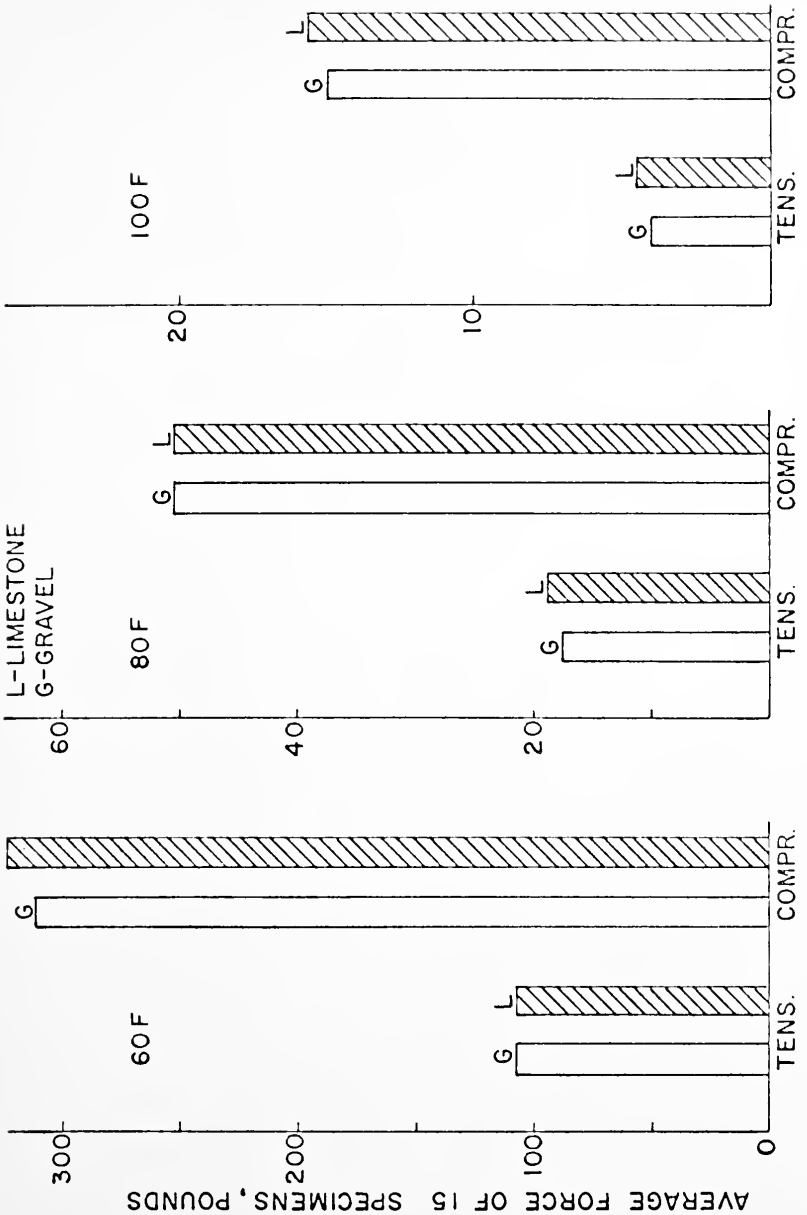

FIGURE 10 FORCE COMPARISONS FOR MIXES IN TENSION AND COMPRESSION, ALL SPECIMENS

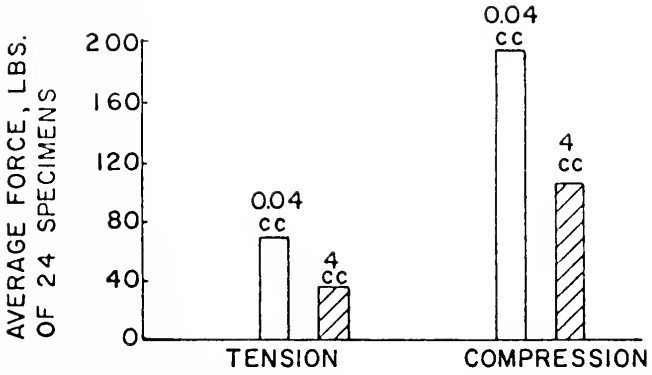

FIGURE 11 FORCE FOR MIXES - 0.04 AND 4CC ROCKS

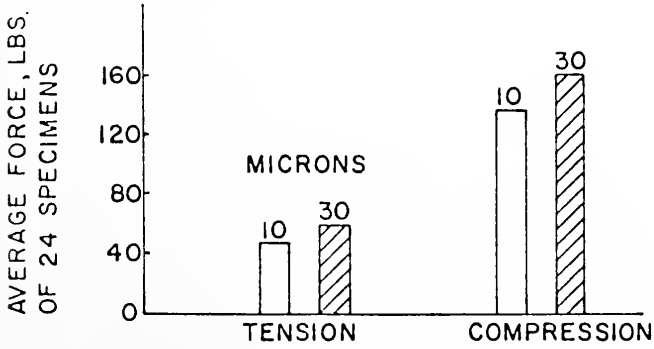

FIGURE 12 FORCE FOR MIXES - 10 AND 30 MICRON FILM

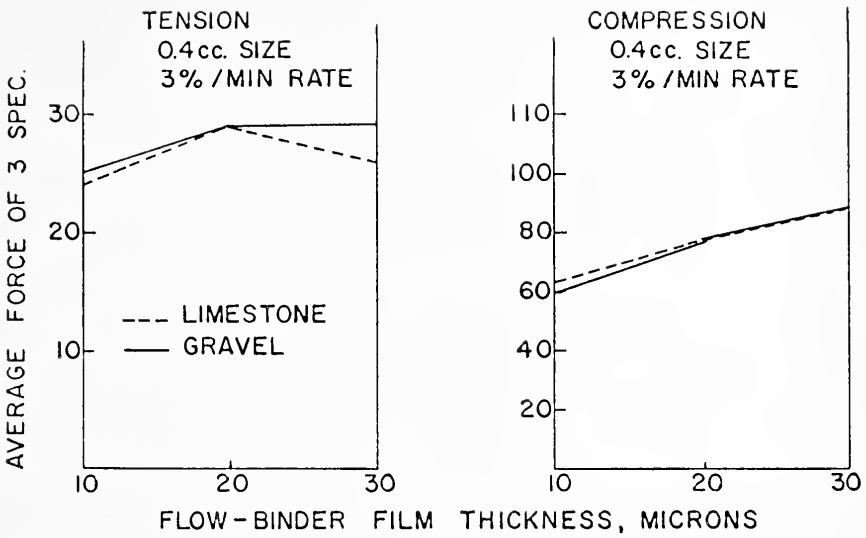

FIGURE 13 FORCE FOR 0.4cc ROCKS AND 3 FILMS

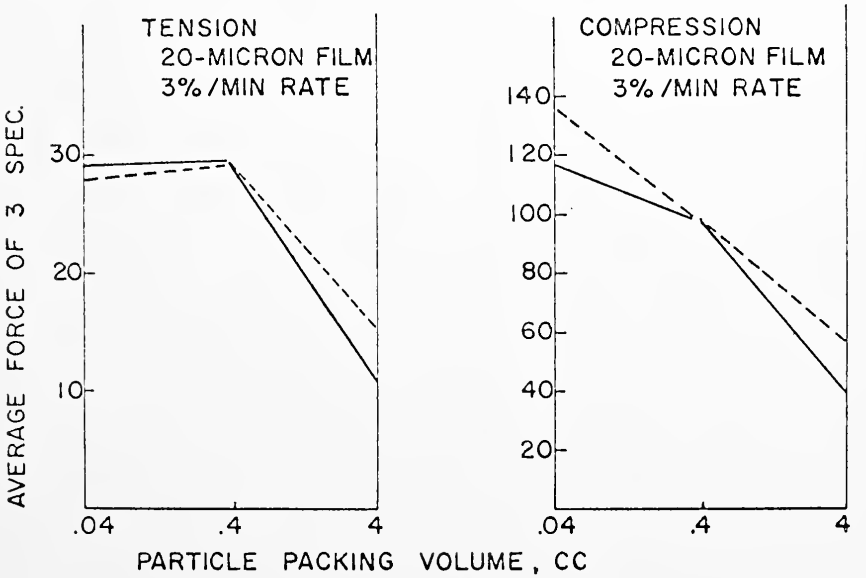

FIGURE 14 FORCE FOR 20 MICRON FILM

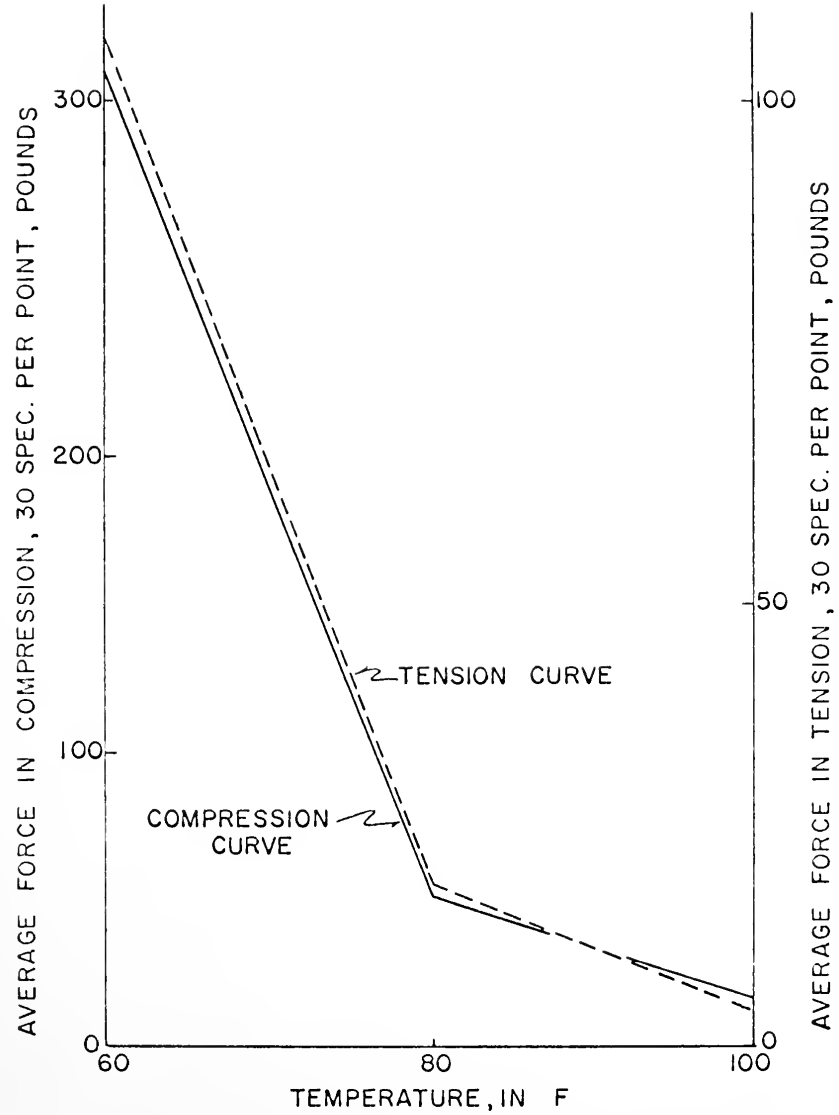

FIGURE 15 FORCE IN COMPRESSION ≈ 3X TENSION

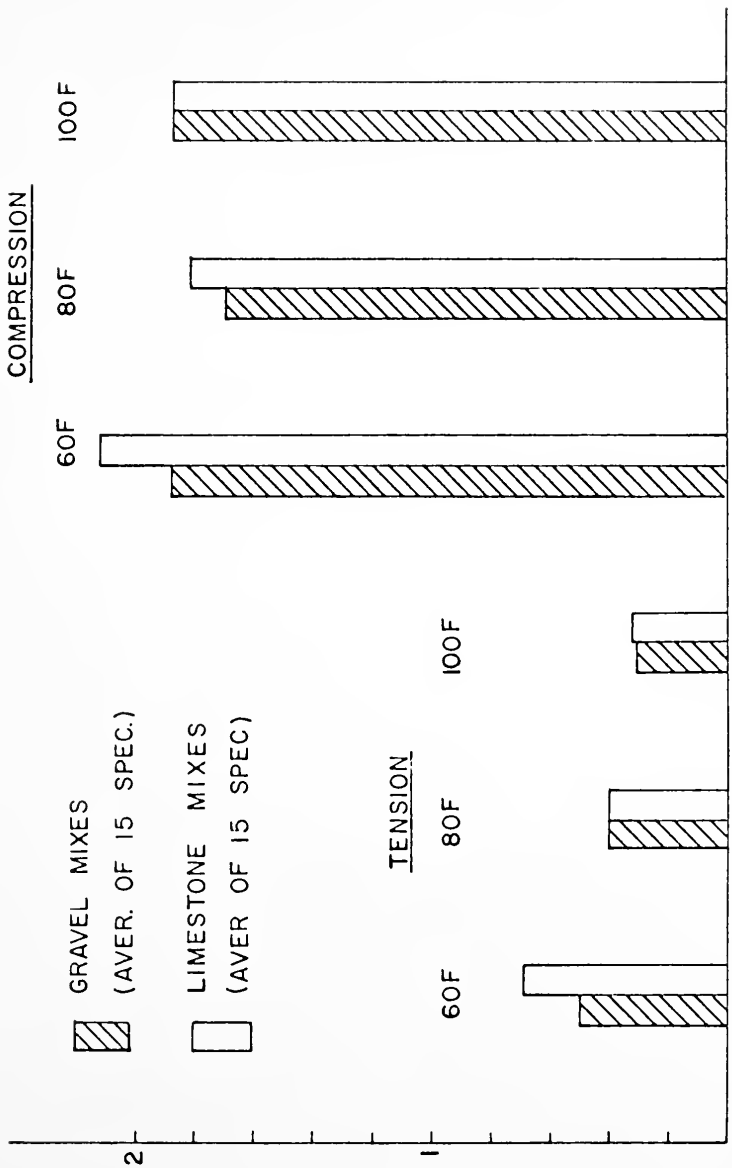

FIGURE 16 AVERAGE VERTICAL STRAIN AT PEAK LOAD

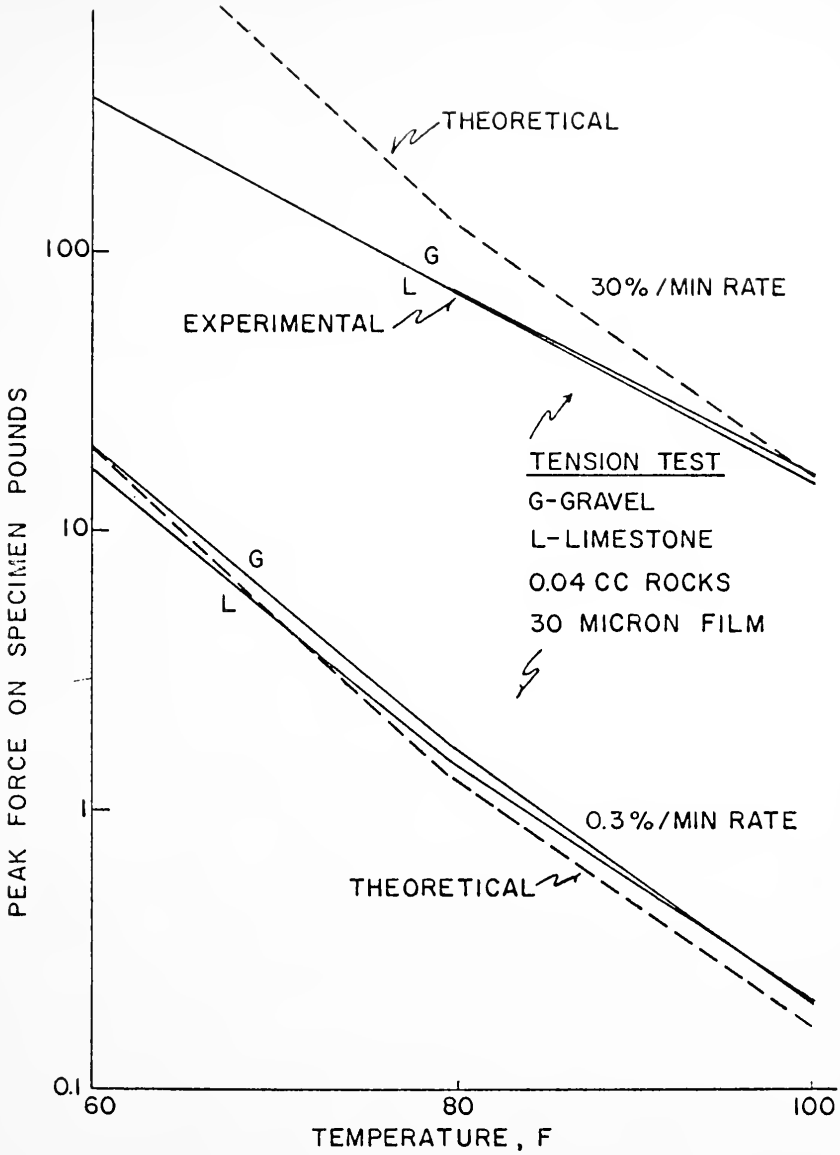

FIGURE 17 THEORETICAL AND EXPERIMENAL TENSILE FORCE, 0.04 CC ROCKS, 30 MICRON FILM

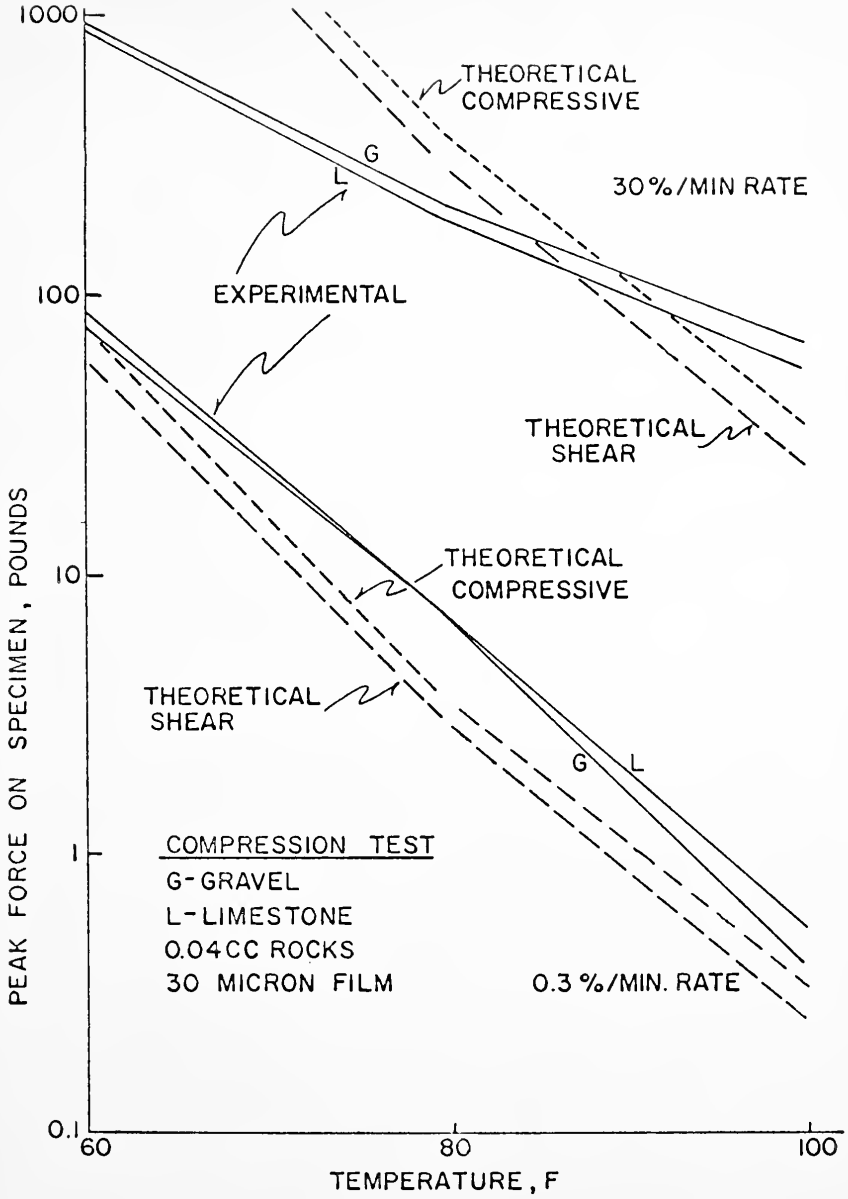

FIGURE 18 EXPERIMENTAL COMPRESSIVE FORCE COMPARED WITH THEORETICAL COMPRESSIVE AND SHEAR FORCES, 0.04 CC ROCKS, 30 MICRON FILM

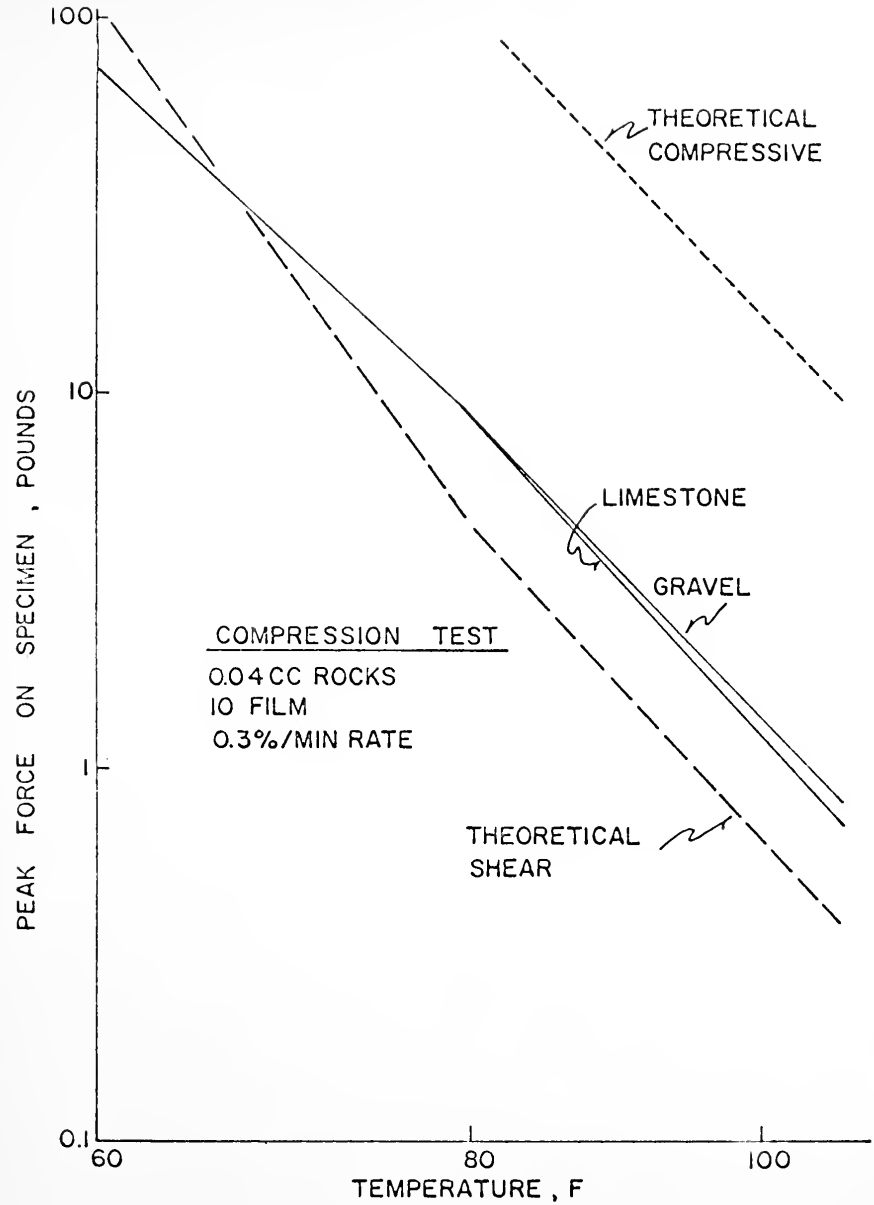

FIGURE 19 EXPERIMENTAL COMPRESSIVE FORCE COMPARED WITH THEORETICAL COMPRESSIVE AND SHEAR FORCES, 0.04CC ROCKS, 0.3%/MIN RATE

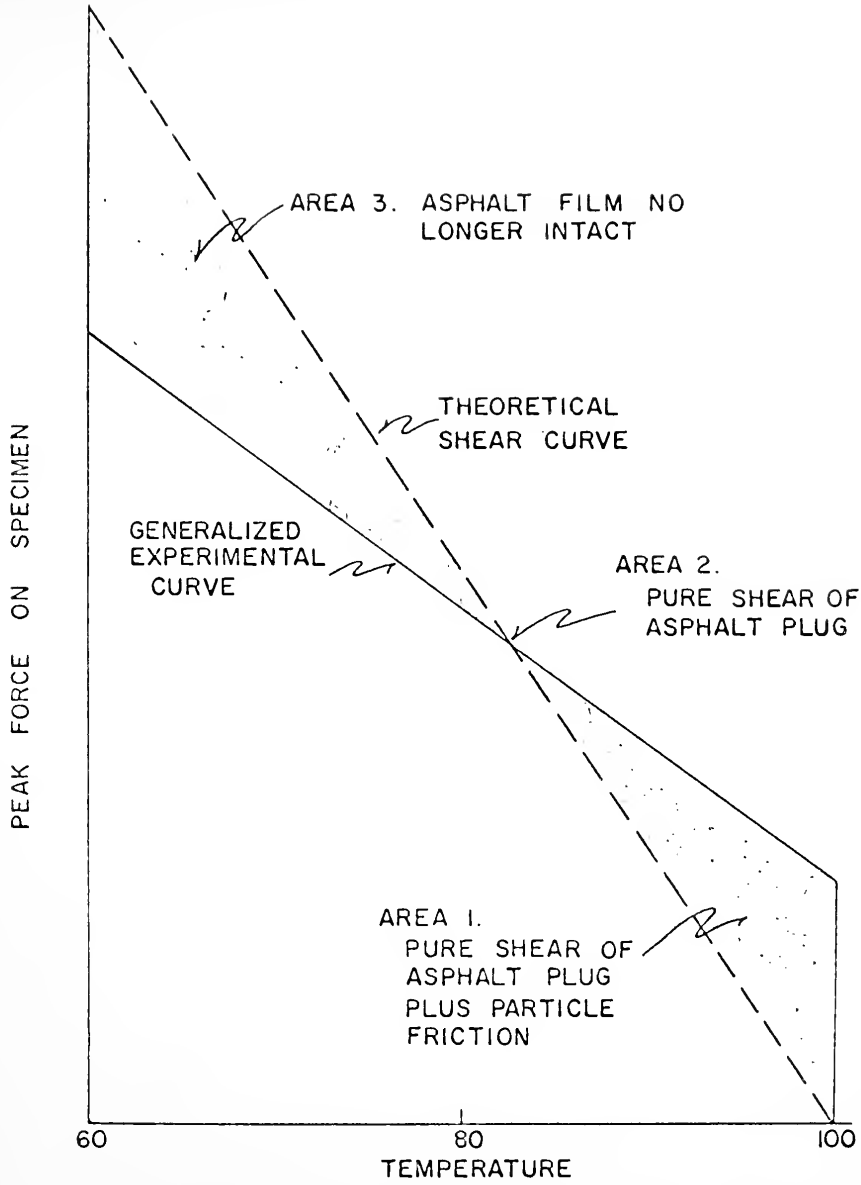

FIGURE 20 CURVES ILLUSTRATING CONCEPTS IN SHEAR FLOW

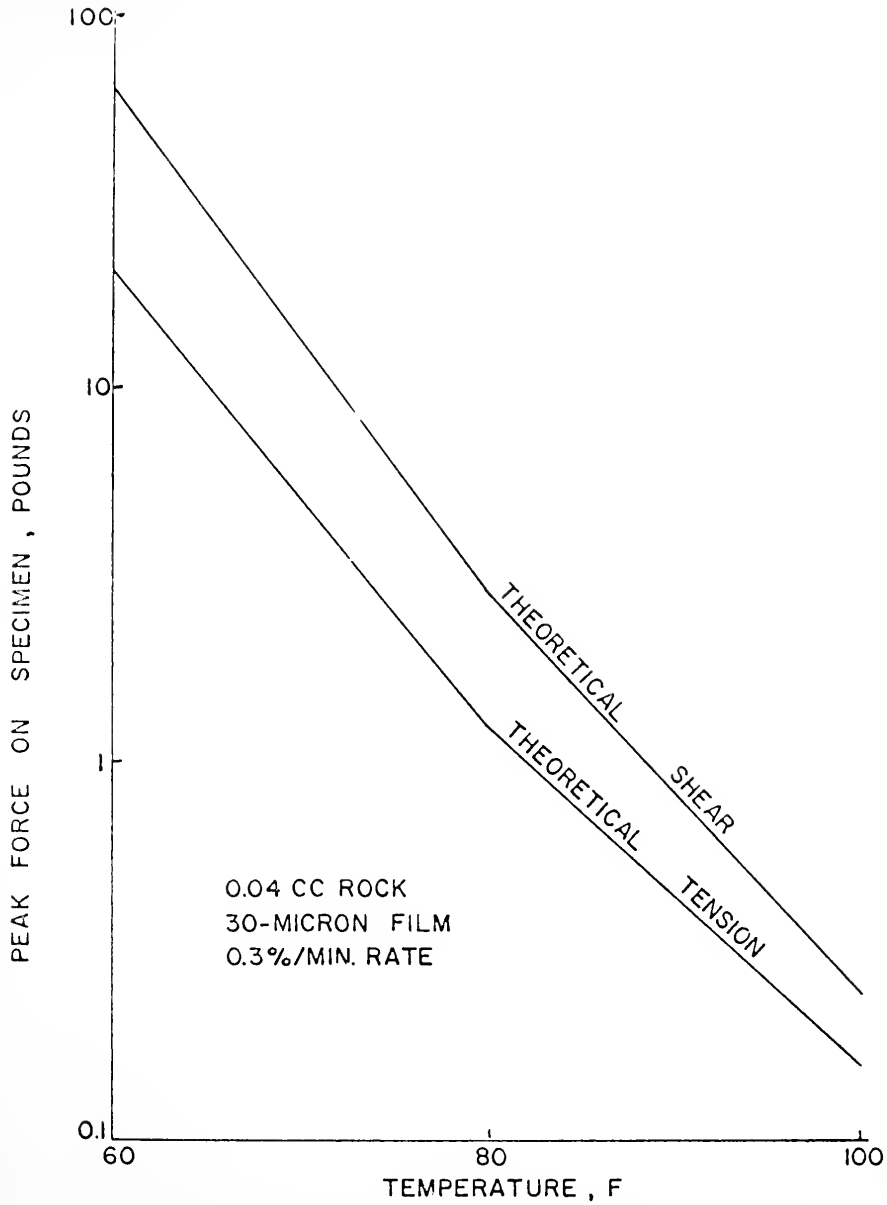

FIGURE 21 THEORETICAL SHEAR AND TENSION CURVES
0.04 CC ROCKS, 30 MICRON FILM, 0.3%/MIN RATE

APPENDIX

CALCULATED VALUES FOR THEORETICAL "STRENGTH"

(a) Size of Contact Radius "r", Microns

	Average Height, h_o, Microns		
	2 x 10 = 20	2 x 20 = 40	2 x 30 = 60
0.04 cc Rocks	310	370	430
0.4 cc Rocks	740	800	857
4 cc Rocks	1430	1520	1600

(b) Values for L and M

	L	M	L/M
0.04 cc Rocks	650	28	23
0.4 cc Rocks	130	13	10
4 cc Rocks	20	4.5	4.5

(c) Sample Calculation of Theoretical Peak Tensile Force for:

0.04 cc rocks
30 - micron film
0.3 %/min. rate
100 F temperature

APPENDIX (continued)

Take Equation 13

$$F_t = \frac{10.73}{10^6}\eta \times \frac{r^4 h_o^2}{(h_o + h)} \times \frac{L}{M} \times \frac{dH}{dt} \quad \text{(Pounds)}$$

$\eta = 1.7 \times 10^5$ poises at 100 F

$r = 430$ microns $= 0.043$ cm

$h_o = 60$ microns $= 0.006$ cm

$\Delta h = \frac{\text{strain at peak force}}{\text{number of films}} = \frac{(0.003)(4)(2.54)}{28} = 0.001$cm

$\frac{L}{M} = 23$

$\frac{dH}{dt} = \frac{(0.003)(4)(2.54)}{60} = 5.08 \times 10^{-4}$ cm/sec

Placing all the values in Equation 13

$$F_t = \frac{(10.73)(1.7)(10)^5(4.3)^4(6^2)(10^{15})(5.08)(23)}{10^6 \quad (10)^8 \quad (10^6)(7)^5 \quad (10^4)} = 0.16 \text{ Pounds}$$

This value is shown in Fig. 17

(d) Sample Calculation of Theoretical Shear Force For:

0.04 cc rocks
30 - micron film
0.3 %/min. rate
100 F temperature

APPENDIX (continued)

Take Equation 15

$$F_s = \frac{2.248}{10^6} \times \eta \times \frac{dx}{dh_o} \times A$$

$\eta = 1.7 \times 10^5$ poises at 100 F

Assuming 45^o sliding angle, shear rate

$$\frac{dx}{dh} = \frac{(5.08)(10^3)(2)}{(10^4)(6)} = 0.17 \text{ sec}^{-1}$$

A = Total asphalt cross-sectional area under shear for 45^o sliding angle

$$A = (3.14)(.043)(.043)(650)(2)$$

Thus finally

$$F_s = \frac{2.248}{10^6} \times \frac{(1.7)(10^5)}{1} \times \frac{(3.14)(4.3)(.43)(650)(2)}{(10)(10^2)} = 0.25 \text{ Pounds}$$

This value is shown in Fig. 18

(c) Sample Calculation of Theoretical Compressive Force

Using Equation 57

$$F_c = \frac{10.73}{10^6} \times \eta \times \frac{r^4}{h_o^3} \times \frac{L}{M} \times \frac{dH}{dt}$$

Calculations are similar to Part C